



## Research article

A sesquiterpene isolated from the stems and leaves of *Dioscorea opposita* Thunb. Transforms the composition of immune cells through ER $\beta$  in a mouse model of LPS-induced lung injury

Mengnan Zeng<sup>a,b,c,1</sup>, Beibei Zhang<sup>a,b,1</sup>, Yingjie Ren<sup>a,b,1</sup>, Shengchao Wang<sup>a,b</sup>, Pengli Guo<sup>a,b</sup>, Meng Liu<sup>a,b</sup>, Qinqin Zhang<sup>a,b</sup>, Jufang Jia<sup>a,b</sup>, Jinyue Li<sup>a</sup>, Xiaoke Zheng<sup>a,b,c,\*</sup>, Weisheng Feng<sup>a,b,c,\*\*</sup>

<sup>a</sup> College of Pharmacy, Henan University of Chinese Medicine, Zhengzhou, China

<sup>b</sup> The Engineering and Technology Center for Chinese Medicine Development of Henan Province, Zhengzhou, China

<sup>c</sup> Collaborative Innovation Center for Respiratory Disease Diagnosis and Treatment & Chinese Medicine Development of Henan Province, Zhengzhou, China

## ARTICLE INFO

## Keywords:

Stems and leaves of *Dioscorea opposita* Thunb.  
Sesquiterpene  
Acute lung injury  
ER $\beta$   
Co-culture system

## ABSTRACT

Acute lung injury (ALI) is a common critical disease with a high mortality rate. Natural products have marked efficacy in the prevention and treatment of ALI, in addition, estrogen and its receptors are involved in the pathogenesis and development of lung injury. Our previous research shows that sesquiterpenes isolated from the stems and leaves of *Dioscorea opposita* Thunb. have anti-inflammatory and estrogenic-like activity. In the present study, sesquiterpene (A1) is a natural extract from the stems and leaves of *Dioscorea opposita* Thunb. with a view to determining whether A1 can improve lung function in a mouse model of LPS-induced ALI and exploring the involvement of the estrogen receptor  $\beta$  (ER $\beta$ ) pathway. A1 (20 or 40 mg/kg, i. g., 2 times/day) was administered for 3 d, followed by the induction of ALI via an intratracheal LPS drip (5 mg/kg/2 h). The lung function and levels of inflammation, immune cells, apoptosis, and ER $\beta$  expression were examined. The antagonistic activity of specific ER $\beta$  blocker (THC, 1  $\mu$ M) against A1 (20  $\mu$ M) in co-cultured BEAS-2B cells and splenic lymphocytes induced with LPS (1  $\mu$ g/mL, 24 h) was also investigated to assess whether the observed effects of A1 were mediated by ER $\beta$ . A1 improved lung function, regulated the immune system, and decreased inflammation and apoptosis. Moreover, A1 increased the expression of ER $\beta$  in LPS-induced mice, and antagonism of ER $\beta$  decreased the protective effects of A1 in a co-culture system. A1 had anti-ALI effects that might partially mediated through ER $\beta$  signaling. Our data provide molecular justification for the use of A1 in the treatment of ALI.

## 1. Introduction

Acute lung injury (ALI) is a severe and progressive respiratory failure that is caused by intrapulmonary and extrapulmonary factors [1]. The main pathogenic feature of ALI is a variety of uncontrolled inflammatory cell-mediated responses that result in damage to the pulmonary blood-gas exchange barrier [2, 3]. In recent years, the mortality rate of ALI has decreased due to continuous in-depth research into the molecular mechanism of the occurrence and development of ALI, as well as the clinical application of treatment measures such as plasma exchange, broad-spectrum antibiotics, and protective ventilation strategies;

however, the mortality rate remains as high as 40% [4, 5]. Effective treatment is still in urgent need and represents an important issue in critical care medicine. Traditional Chinese medicine (TCM) research has become increasingly popular [6, 7, 8], and studies have shown that a variety of natural compounds extracted from such plants can effectively regulate ALI. For example, Lan *et al.* found that salidroside can reduce the content of some pro-inflammatory factors, such as tumor necrosis factor- $\alpha$  (TNF- $\alpha$ ), nitric oxide (NO) and interleukin-6 (IL-6), in mice with ALI [9]. Shi *et al.* demonstrated that injections composed of rutin, chlorogenic acid, and ferulic acid can regulate ALI by participating in the metabolism of fatty acids, amino acids, and purines in mice with ALI

\* Corresponding author.

\*\* Corresponding author.

E-mail addresses: [zhengxk.2006@163.com](mailto:zhengxk.2006@163.com) (X. Zheng), [fwsh@hactcm.edu.cn](mailto:fwsh@hactcm.edu.cn) (W. Feng).

<sup>1</sup> These authors contributed equally to this work.

[10]. Owing to gradual improvement in the understanding of TCM, extracted active ingredients displaying significant therapeutic effects and low toxicity have begun to attract attention.

*Dioscorea opposita* Thunb. was first recorded in “Shen Nong’s Materia Medica” and was regarded as a typical example of “ingredients as both medicine and food” in ancient China. In traditional TCM books, its efficacies include promoting body fluids, nourishing the lungs, tonifying the kidneys, and improving male sexual function [11]. Modern medical research has shown that *Dioscorea opposita* Thunb. displays anti-inflammatory and anti-tumor activities [12]. Nevertheless, during the harvesting process of *Dioscorea opposita* Thunb., its non-medicinal parts (stems and leaves) accumulate in fields, causing environmental pollution and excess waste. At present, many non-medicinal parts of TCM plants or their extracts are used clinically. For example, *Eucommia ulmoides* leaves are low-cost and possess antihypertensive effects [13]; chlorogenic acid extracted from these leaves displays antibacterial and anti-inflammatory efficacies [14]. Our previous research shows that sesquiterpenes and diphenylethanes isolated from the stems and leaves of *Dioscorea opposita* Thunb. have estrogenic-like activity (mediated by the estrogen receptor (ER)) [15, 16]. We also found that *Dioscorea opposita* Thunb. extract attenuated LPS-induced cardiac dysfunction by inhibiting RAS and apoptosis via the ER-mediated activation of SHC/Ras/Raf1 pathway [17]. Related studies have demonstrated that estrogen can alleviate ALI through ER signaling and accordingly, women are more likely to resist damage to organs caused by external stimuli, which indicates that ER signaling may play an important role in the treatment of ALI [18]. In the present study, a high-content sesquiterpenoid was isolated from the stems and leaves of *Dioscorea opposita* Thunb. and its intervention in ALI was investigated from the perspective of ER signaling.

## 2. Materials and methods

### 2.1. Preparation of A1

The dried stems and leaves of *Dioscorea opposita* Thunb (voucher specimen No. 20171115A) were collected in September 2017 from Jiaozuo city, Henan province, People’s Republic of China. Extraction and isolation of the stems and leaves of *Dioscorea opposita* Thunb. were performed as previously reported [15]. Here, A1 (964.21 mg) was obtained from the CH<sub>2</sub>Cl<sub>2</sub> fraction. The Yield of A1 was 0.024%. The data added in supplementary material 1.

### 2.2. Animal experiments

Male Balb/c mice were used in the present study, with operating specifications as previously reported [19]. The study was conducted in accordance with the Experimental Animal Administration regulations issued by the State Committee of Science and Technology of the People’s Republic of China. All procedures were performed in accordance with the Guidelines for Care and Use of Laboratory Animals of Henan University of Chinese Medicine, and the experiments were approved by the Animal Ethics Committee of Henan University of Chinese Medicine (DWLL2018080003, 2018.08.15–2023.08.15). Mice were fit with an intratracheal LPS drip (M, 5 mg/kg, excluding the control group) and subjected 2 h later to gavage with Vitamin E (VE, positive control, 30 mg/kg) or different doses of A1 (Low, 20 mg/kg; High, 40 mg/kg), 6 per group, which continued twice a day for 3 day [20]. The other groups were orally administered the same volume of distilled water. The heart and lung functions of the mice were evaluated using a small-animal ultrasound system (VISUAL SONICS, FUJ. FILM, Japan). Lung tissue and blood were removed immediately.

### 2.3. Near-infrared in vivo imaging

Mice were fit with an intratracheal LPS drip (5 mg/kg), injected 2 h later with the IRDye® 800 C W 2-DG Optical Probe (mice in all groups as

above, 10 nmol/25 g), and subjected to gavage with VE or different doses of A1, 3 per group, twice a day for 3 days. Mouse anesthesia by isoflurane, near-infrared imaging, and analysis were performed as described in the literature [21].

### 2.4. Histological examination and immunohistochemical staining

Lung tissues were fixed in 4% paraformaldehyde and sectioned at a thickness of 5 μm [22]. Hematoxylin and eosin (H&E) and Sirius Red staining was performed according to standard protocols, and slides were viewed under a microscope (Nikon, Japan). Moreover, sections were incubated at 4 °C overnight with a primary antibody (anti-cleaved caspase-3 ab32042, Abcam, USA), followed by a secondary antibody (indirect fluorescence staining) for 2 h at room temperature. Nuclei were stained with 4,6-diamino-2-phenyl indole (DAPI). Images were examined and scanned under an optical microscope (XSP-C204, CIC, Chongqing, China). Using Image Pro-Plus software, the lumen thickness and integrated optical density were statistically analyzed (5 pictures per animal).

In addition, 5-μm cryosections were dehydrated in 100% ethanol and rehydrated in decreasing concentrations of ethanol in antigen retrieval solution (G1206, Servicebio, China). After treatment with Protein Block Serum-Free (Agilent), sections were incubated overnight at 4 °C with primary antibodies against the following proteins: cluster of differentiation (CD) 31 (Cat no. GB13428), ERβ (GB11514), and interleukin-1β (IL-1β, GB11113) (Servicebio, China). The next day, sections were treated with the corresponding fluorescently labeled secondary antibodies (GB23303, GB22303, and GB27303, respectively; Servicebio, China) for 1 h at 25 °C and subsequently mounted with VECTASHIELD Mounting Medium containing DAPI. Fluorescent images were acquired using the Nikon Eclipse C1 and Nikon DS-U3 systems (Nikon, Japan).

### 2.5. Transmission electron microscopy

Small fragments of lung tissue were fixed in glutaraldehyde and osmic acid, dehydrated with graded ethanol, and embedded in ethoxyline resin. Sections were cut to a thickness of 70–80 nm and viewed under a transmission electron microscope (TEM) (JEM-1400, JEOL, Japan).

### 2.6. Western blotting

The protein expression levels of IL-1β and ERβ were detected by western blotting. The protein samples were separated by sodium dodecyl sulfate-polyacrylamide gel electrophoresis (SDS-PAGE) (Bio-Rad, USA) and transferred to polyvinylidene fluoride (PVDF) membrane. The membranes were incubated with primary antibodies (IL-1β, ab9722 Abcam, 1:2000; ERβ, ab3576 Abcam, 1:2000) overnight at 4 °C, followed by a secondary antibody (goat anti-rabbit 925–68071, Li-COR, MO, USA), 1:10000 for 1 h at room temperature. Densitometric quantitation of the protein bands was performed using Odyssey (Clx, Li-COR).

### 2.7. Co-culture of BEAS-2B cells and splenic lymphocytes

Lung epithelial cells (BEAS-2B) were obtained from Shanghai Cell Bank of Chinese Academy of Sciences and splenic lymphocytes were isolated from spleens. Co-culture of BEAS-2B cells (2×10<sup>6</sup>) and splenic lymphocytes (1×10<sup>7</sup>) was performed as described previously [23, 24]. The present study comprised 12 groups: (1) control (BEAS-2B cells, 2×10<sup>6</sup>); (2) control + splenic lymphocytes (1×10<sup>7</sup>); (3) model (BEAS-2B cells, 2×10<sup>6</sup>; LPS 1 μg/mL); (4) model + splenic lymphocytes; (5) model + A1 (20 μM); and (6) model + A1 + splenic lymphocytes. In addition, THC (1 μM, specific ERβ blocker) was added 30 min prior to the above treatments in groups 7–12 to assess whether the observed influences of A1 or splenic lymphocytes were mediated by ERβ. After 24 h, the supernatant was collected from each group and analyzed by enzyme-linked immunosorbent assay (ELISA); BEAS-2B cells were collected from each group and evaluated by the Annexin V/PI double-staining apoptosis

assay; and splenic lymphocytes were collected and examined by flow cytometry.

### 2.8. Flow cytometry analysis of immune cells

The cells ( $4 \times 10^5$  splenic lymphocytes from co-culture or spleens, or  $4 \times 10^5$  cells from blood) were resuspended in 100  $\mu$ L PBS [22]. Helper (Th) and cytotoxic (Tc) cells were detected by antibodies against CD3/4/8. Dendritic cells (DCs) were examined by anti-CD11c and anti-CD86 antibodies. NK cells were detected by anti-CD3e and anti-CD49b antibodies. MDSCs were examined by anti-CD11b and anti-Ly-6G antibodies. Regulatory T cells (Tregs) were detected by anti-CD4, anti-CD25, and anti-Foxp3 antibodies. All antibodies were purchased from ThermoFisher (USA) and used according to the manufacturer's instructions. Flow cytometry (FACS Aria III, BD Biosciences, USA) was used to detect the cellular fluorescence intensity.

### 2.9. Apoptosis assay

The apoptosis of BEAS-2B cells was assessed by Annexin V/PI according to the manufacturer's instructions (BD Biosciences 556547, USA).

### 2.10. ELISA

Serum, alveolar lavage fluid, or cell supernatant were collected and used to detect the levels of IL-6 (E-EL-M0044c, Elabscience Co., Ltd., Wuhan, China), TNF- $\alpha$  (E-EL-M0049c, Elabscience Co., Ltd., Wuhan, China), interleukin 17 (IL-17; E-EL-M0047c, Elabscience Co., Ltd., Wuhan, China), and interferon  $\gamma$  (IFN- $\gamma$ ; E-EL-M0048c, Elabscience Co., Ltd., Wuhan, China), according to the respective manufacturer's protocol.

### 2.11. Molecular docking

The Sybyl/Surflex module was employed to investigate the potential interactions between ER $\beta$  and A1. The ER $\beta$  protein was used as the receptor (PDB: 1U3Q) and A1 was obtained from the website (<http://zinc15.docking.org>). All docking simulations were performed using default parameters, and binding affinities were estimated by total scores. The docking results were further visualized with a 2D/3D molecular descriptor using the Discovery Studio Visualizer software.

### 2.12. Statistical analysis

Data were analyzed using SPSS 20.0 (IBM, NY, USA). Statistical significance was assessed in comparison with the respective control for each experiment using one-way analysis of variance (ANOVA), least significant difference test (LSD) was used for data with homogeneous variance, and Games-Howell was used for non-homogeneous variance. *P* values less than 0.05 were accepted as significant.

## 3. Results

### 3.1. A1 inhibits LPS-induced acute lung injury in mice

Lung function was assessed by measuring the PAAT (pulmonary arterial acceleration time) and PET (pulmonary arterial ejection time). The results of animal ultrasound demonstrate that PAAT and PET were reduced in the model group (intratracheal LPS drip, 5 mg/kg) and significantly reversed following VE or A1 treatment (Figure 1A). Moreover, LPS (intratracheal drip) and A1 had a slight effect on the heart function (LVEF, left ventricular ejection fraction; LVFS, left ventricular fraction shortening) of mice (Figure 1B). H&E staining shows that epithelial injury (Figure 1C, red circle), airway wall thickening (Figure 1C, yellow line), and inflammatory cell infiltration of lung parenchyma (Figure 1C, blue arrow) were greater in the model group. In

contrast, VE or A1 treatment reversed the LPS-induced injury of lung epithelial cells to mild.

The ultrastructure of pulmonary blood vessels indicates that pulmonary vascular endothelium (Ed) edema was increased, the number of mitochondria (Mi) were decreased, the connections of pulmonary capillaries were widened, and the basal membrane (BM) was thickened in the model group, indicating that endothelial cells were in the injury stage (Figure 1D). In addition, the internal elastic lamina (IEL) in the model group was thin and broken, and the smooth muscle cells (SMC) were blurred (Figure 1E). As expected, VE or A1 treatment attenuated these phenomena (Figure 1E and D). Consistent with the results of animal ultrasound and H&E staining, A1 had a significant protective effect on lung function.

Caspase-3 is a marker of apoptosis and accordingly, immunofluorescence was used to evaluate whether A1 affected apoptosis *in vivo*. As shown in Figure 1F, increased expression of cleaved caspase-3 was found in the model group as compared with that in the control group; however, this expression was significantly reduced in the VE- and A1-treated groups.

### 3.2. A1 inhibits the LPS-induced inflammatory response in mice

To quantitate and assess the efficacy of A1, a 2-DG optical probe was employed as described previously [19]. As shown in Figure 2A, the fluorescence intensity in the LPS group (mice and lungs) was significantly increased, whereas the fluorescence intensity in the A1-treated groups was significantly decreased ( $p < 0.01$ ). At the same time, the levels of TNF- $\alpha$ , IL-6, IFN- $\gamma$ , and IL-17 in the serum and lung tissue were measured. As shown in Figure 2B and C, the levels of these cytokines were significantly increased in the LPS group; however, administration of VE or A1 markedly reversed the LPS-induced upregulation of these inflammatory factors.

### 3.3. A1 increases the percentage of immune cells in the mouse spleen and blood

Knowledge of host cell-mediated immunity is essential for an in-depth understanding of the pathological process of organ damage. Research demonstrates that innate immune cells maintain the body's internal balance and play a vital role in regulating the immune response. To investigate the effect of A1 on the number of immune cells, flow cytometry was employed. A1 significantly increased the percentage of Th cells, Tc cells, DCs, and NK cells in a dose-dependent manner, and decreased the percentage of MDSCs and Tregs in both the mouse spleen and blood as compared with model mice (intratracheal LPS drip, 5 mg/kg), while VE only slightly changed the percentage of these subgroups (Figures 3 and 4). These findings suggest that A1 has excellent immunoregulatory efficacy.

### 3.4. A1 down-regulates CD31 and IL-1 $\beta$ while up-regulates ER $\beta$

To observe the anti-angiogenic effect of A1, lung tissues were stained with an anti-CD31 (an endothelial cell marker) antibody. As shown in Figure 5A, fewer CD31<sup>+</sup> lung microvessels were seen in the VE and A1-treated groups. In addition, immunofluorescence shows that A1 significantly increased the expression of ER $\beta$  and decreased the expression of IL-1 $\beta$  (Figure 5A). Consistent with these results, western blotting indicates that A1 upregulated the expression of ER $\beta$  and downregulated the expression of IL-1 $\beta$  in lung tissues (Figure 5B, non-adjusted images as supplementary material 1). To further investigate their molecular interaction, ER $\beta$  (PDB: 1U3Q) and A1 were subjected to molecular simulation. As shown in Figure 5C, two H-bonds and eight hydrophobic interactions occurred between A1 and the active pocket of ER $\beta$ , suggesting that A1 is a potential ER $\beta$  agonist.

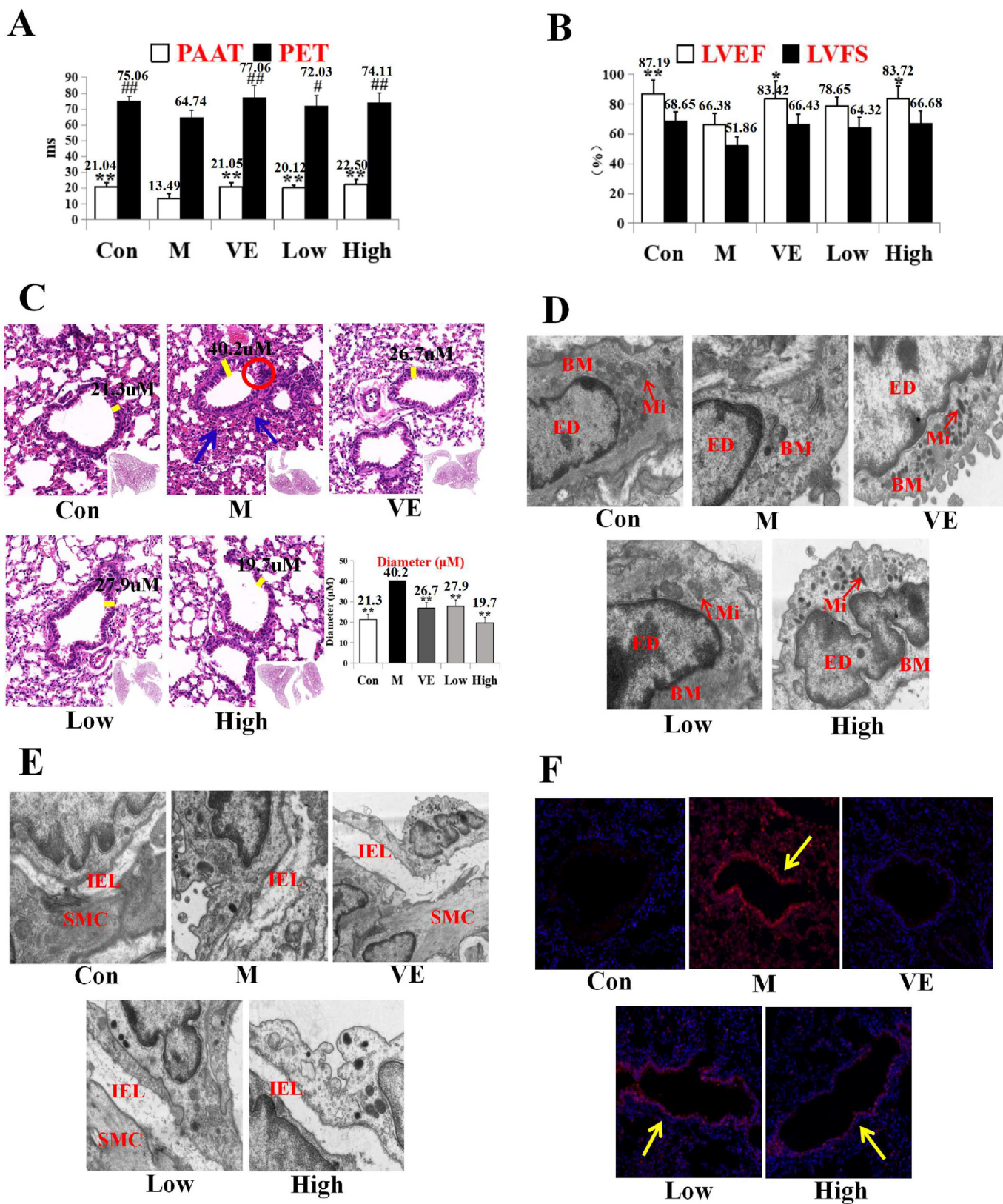


**Figure 1.** A1 inhibits LPS-induced lung injury in mice. A1 (Corchoinol C) was administered after intratracheal LPS drip (5 mg/kg), heart and lung function were detected by animal ultrasound, and the organs were extracted. A: PAAT and PET. B: LVEF and LVFS. C: H&E staining of lung tissues (40× magnification). D: Changes in capillaries under electron microscopy. E: Changes in IEL under electron microscopy. F: Expression of cleaved caspase-3. Data are presented as mean ± SD of 6 mice. \**p* < 0.05, \*\**p* < 0.01 vs. model group; #*p* < 0.05, ##*p* < 0.01 vs. model group (Figure 2A, PET).

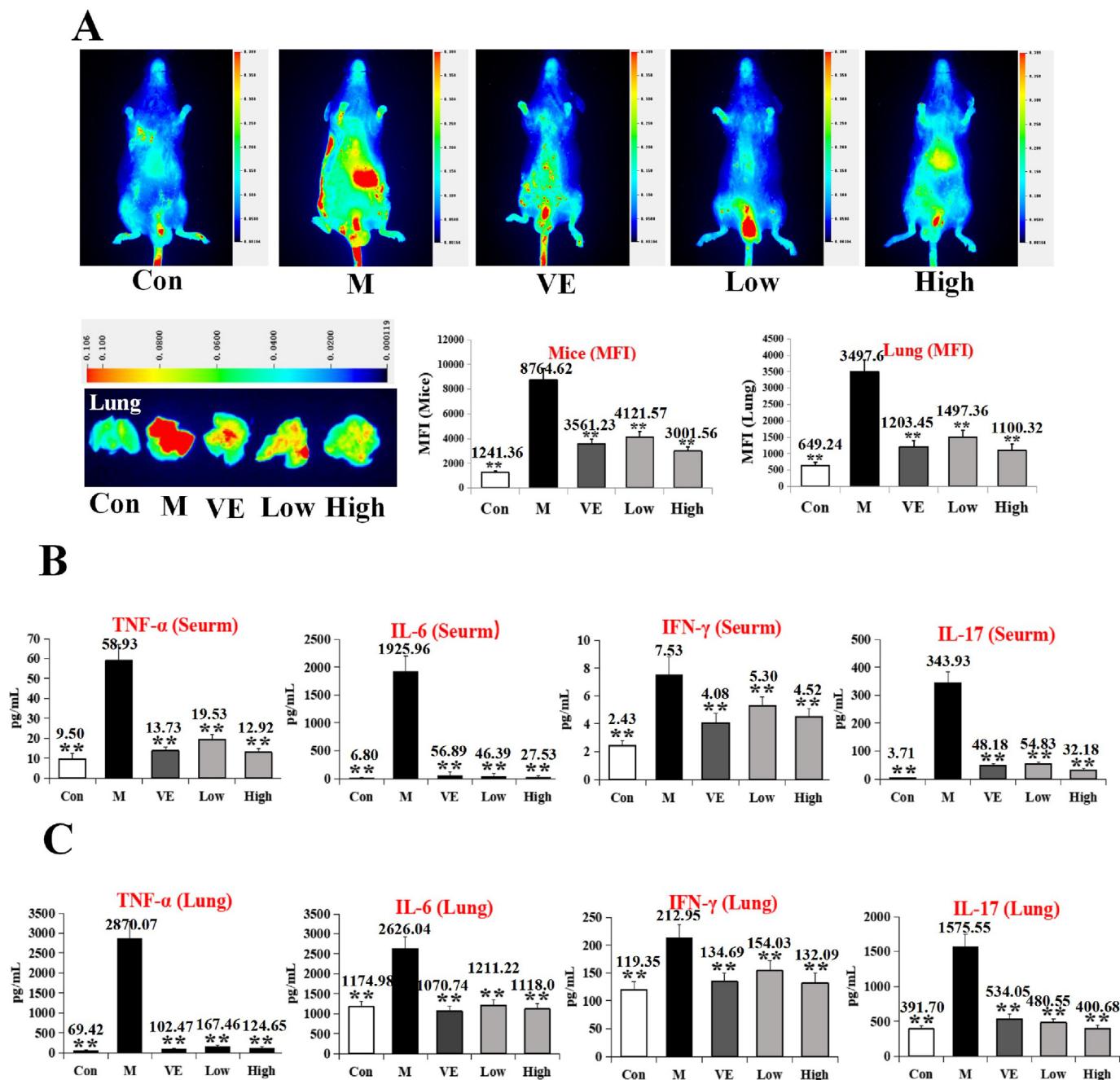


**Figure 2.** A1 (Corchoionol C) inhibits the LPS-induced inflammatory response in mice. Mice were fit with an intratracheal LPS drip, 2 h later, injected with IRDyes 800 C W 2-DG Optical Probe. 18 h after the last administration, near-infrared imaging was performed. A: 2-DG optical probe imaging of A1. B: The levels of inflammatory factors in serum. C: The levels of inflammatory factors in lung tissue. Data are presented as mean ± SD of 3/6 mice. \**p* < 0.05, \*\**p* < 0.01 vs. model group.

**3.5. A1 reprograms the microenvironment through ERβ in a co-culture system**

Flow cytometry shows that A1 increased the percentage of Th and Tc cells and decreased the apoptosis of BEAS-2B cells in the co-culture system (Figure 6B and C). The supernatant was collected and the levels of the proinflammatory cytokines, IL-6 and TNF-α, were measured by ELISA. As shown in Figure 6A, the levels of IL-6 and TNF-α in the co-culture system were significantly reduced by A1.

To determine the role of ERβ in the effect of A1 on the injured lung microenvironment, we blocked ERβ in the co-culture system using THC (a specific ERβ antagonist). The ELISA results show that blockade of ERβ diminished the ability of A1 to lower the levels of IL-6 and TNF-α

(Figure 6A). As shown in Figure 6B and C, the flow cytometry results show that blockade of ERβ attenuated the A1-induced increase in the percentage of Th and Tc cells and the decrease in the percentage of apoptosis of BEAS-2B cells. Taken together, these data demonstrate that blockade of ERβ diminished the influence of A1 on the injured lung microenvironment. In addition, a schematic diagram showing the effects of A1 in LPS-induced ALI (Figure 7).

**4. Discussion**

ALI is a critical illness commonly seen in the clinic, the incidence and lethality of which are increasing annually. In essence, ALI is an unbalanced inflammatory response that causes diffuse alveolar and pulmonary

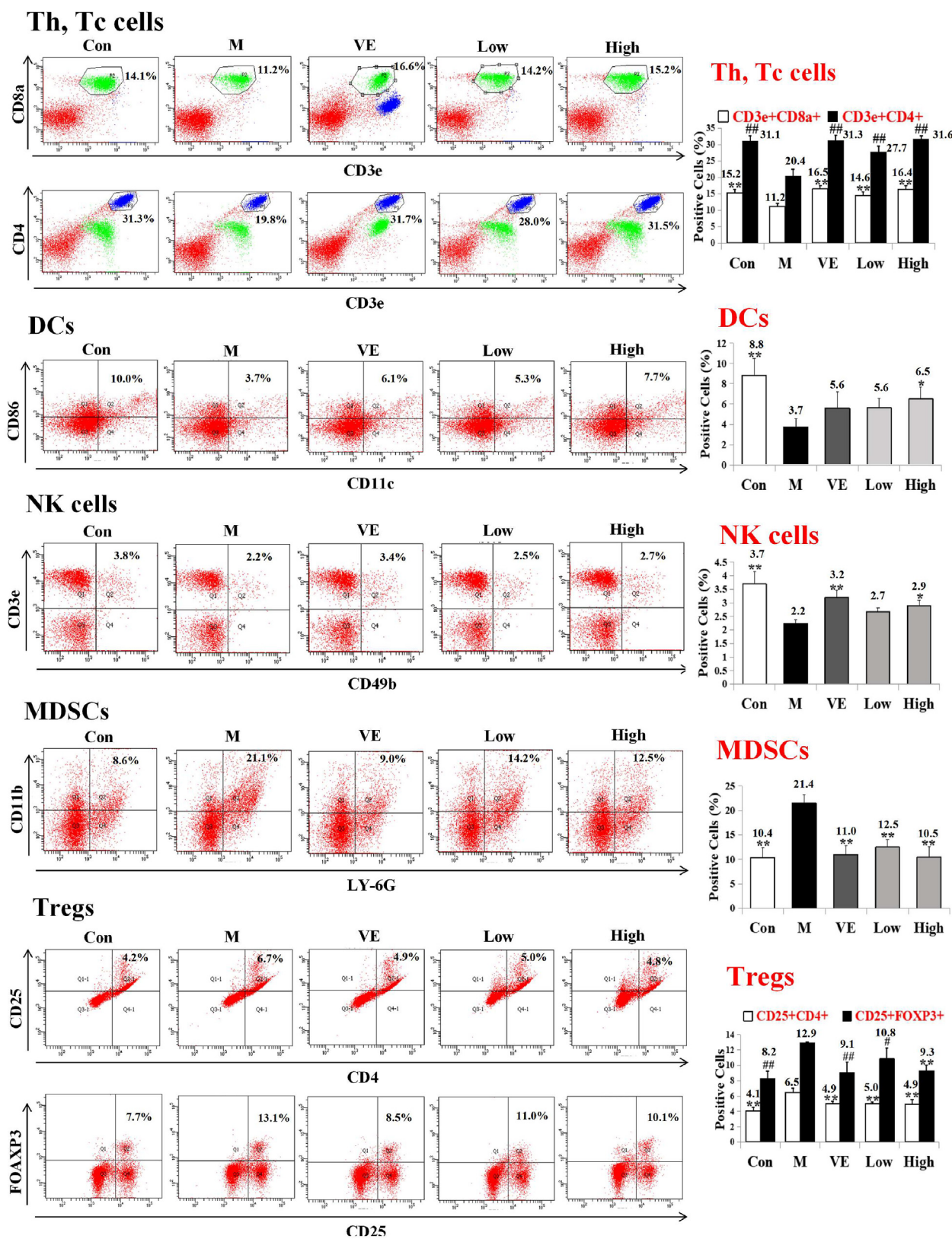


**Figure 3.** A1 (Corchoionol C) alters the percentage of immune cells in the spleen. A1 was administered after intratracheal LPS drip (5 mg/kg), immune cells in the spleen were analyzed by flow cytometry. Representative results of three independent experiments were shown, data are presented as mean ± SD; \**p* < 0.05, \*\**p* < 0.01 vs. model group.

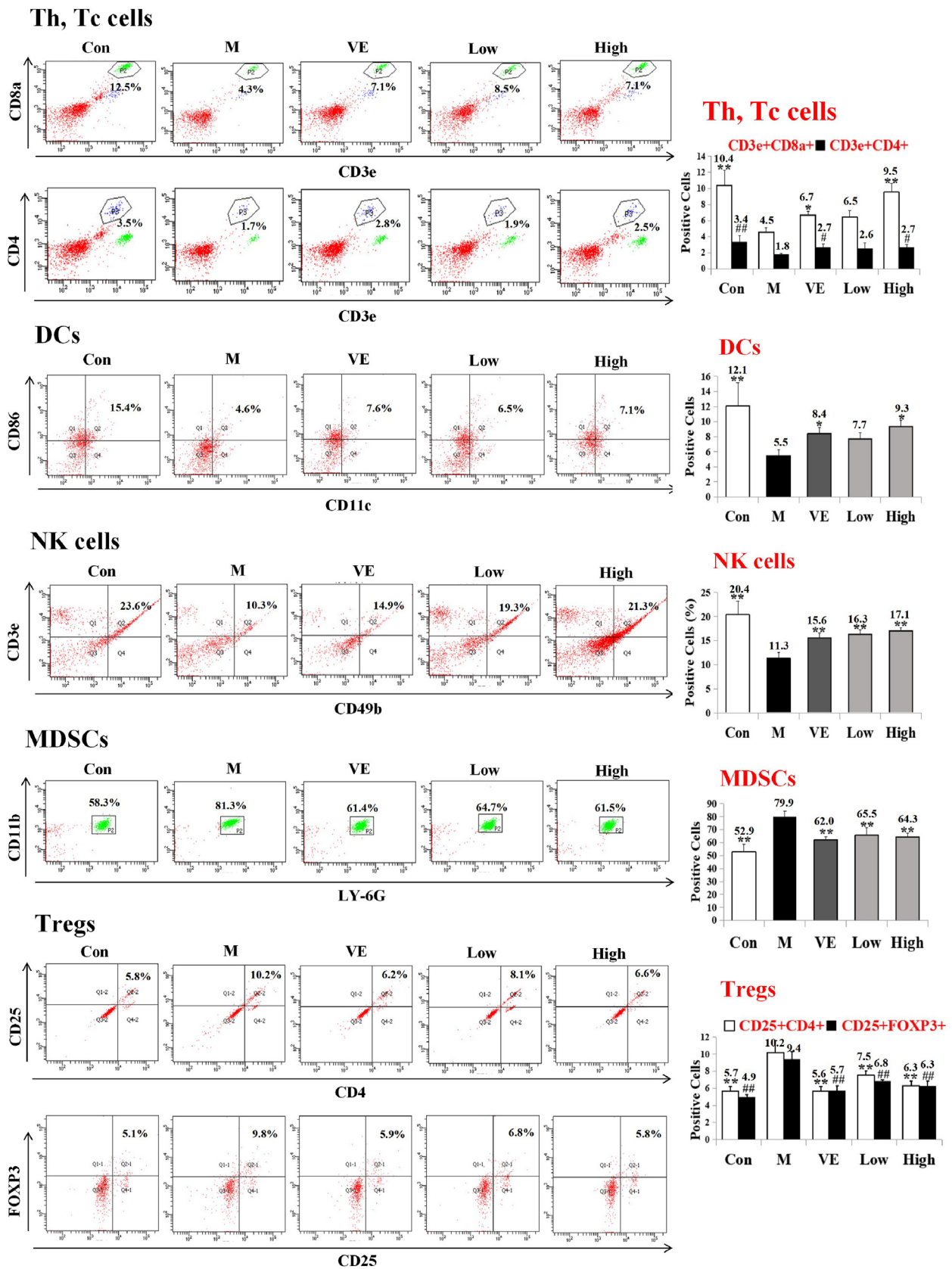


**Figure 4.** A1 (Gorchoionol C) alters the percentage of immune cells in the blood. A1 was administered after intratracheal LPS drip (5 mg/kg), immune cells in the blood were analyzed by flow cytometry. Representative results of three independent experiments were shown, data are presented as mean  $\pm$  SD; \* $p$  < 0.05, \*\* $p$  < 0.01 vs. model group.

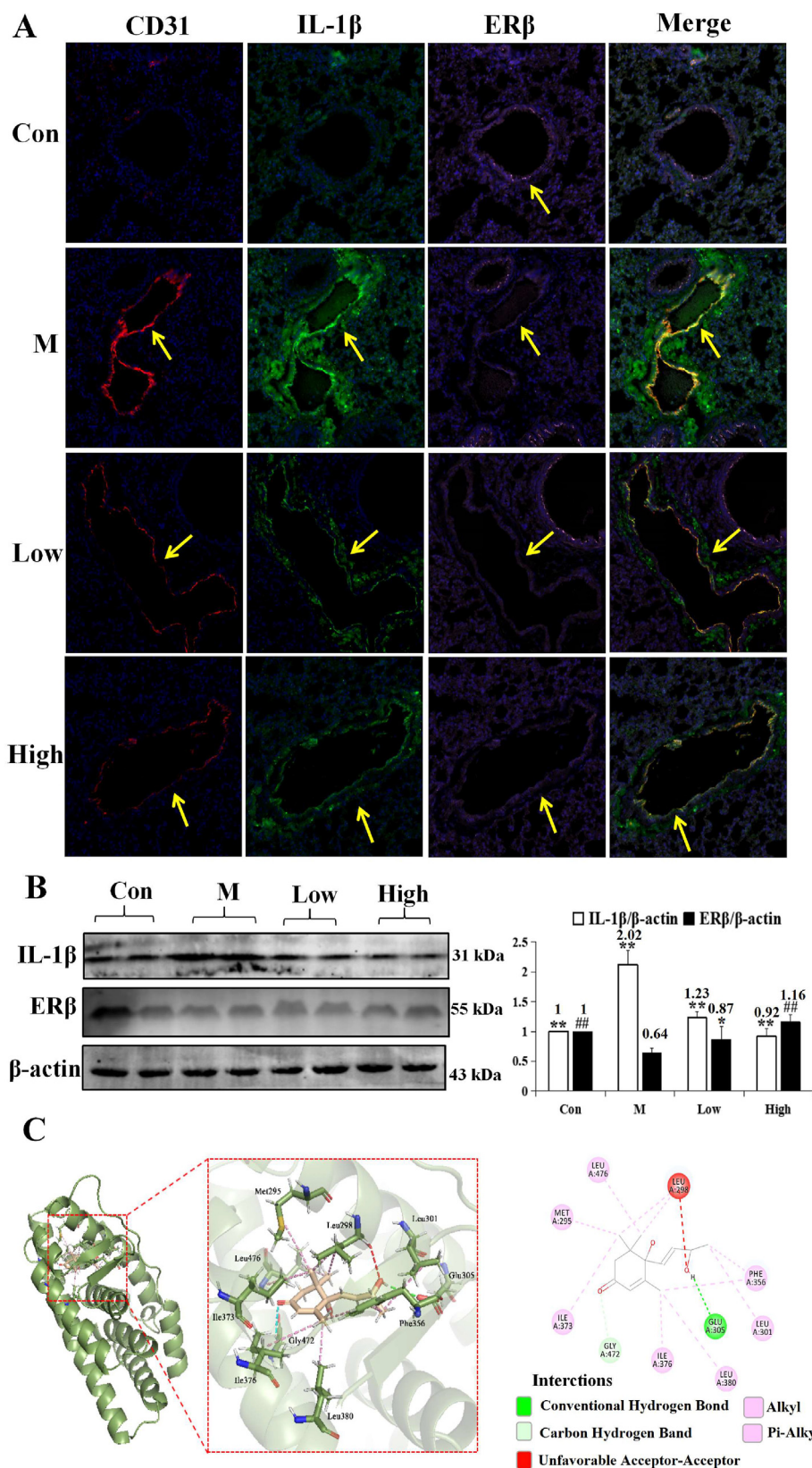


**Figure 5.** A1 (Corchoinol C) down-regulates CD31 and IL-1 $\beta$  while up-regulates ER $\beta$ . A1 was administered after intratracheal LPS drip (5 mg/kg), immunofluorescence and western blotting were used to detect the levels of CD31, IL-1 $\beta$ , and ER $\beta$ . Molecular docking simulated the binding mode of A1 and ER $\beta$ . A: Immunofluorescence. B: Western blotting. C: The binding mode of A1 and ER $\beta$ . Representative results of three independent experiments were shown, data are presented as mean  $\pm$  SD; <sup>\*</sup> $p$  < 0.05, <sup>\*\*</sup> $p$  < 0.01 vs. model group (IL-1 $\beta$ / $\beta$ -actin); <sup>#</sup> $p$  < 0.05, <sup>##</sup> $p$  < 0.01 vs. model group (ER $\beta$ / $\beta$ -actin).

endothelial cell damage, lung tissue edema, and other pathological features. Currently, hundreds of factors are known to induce ALI occurrence directly or indirectly, among which Gram-negative bacillus infection is the most common cause in clinical practice [27]. Accordingly, endotoxin is the most commonly used method in the laboratory to prepare animal

models of ALI. Worldwide, treatment strategies for ALI mainly include reducing inflammation and suppressing respiratory failure with the use of aspirin, salbutamol, and ketoconazole, or respiratory support (e.g., with a ventilator); however, the mortality rate of ALI remains high. In recent years, an increasing number of reports have been published on the



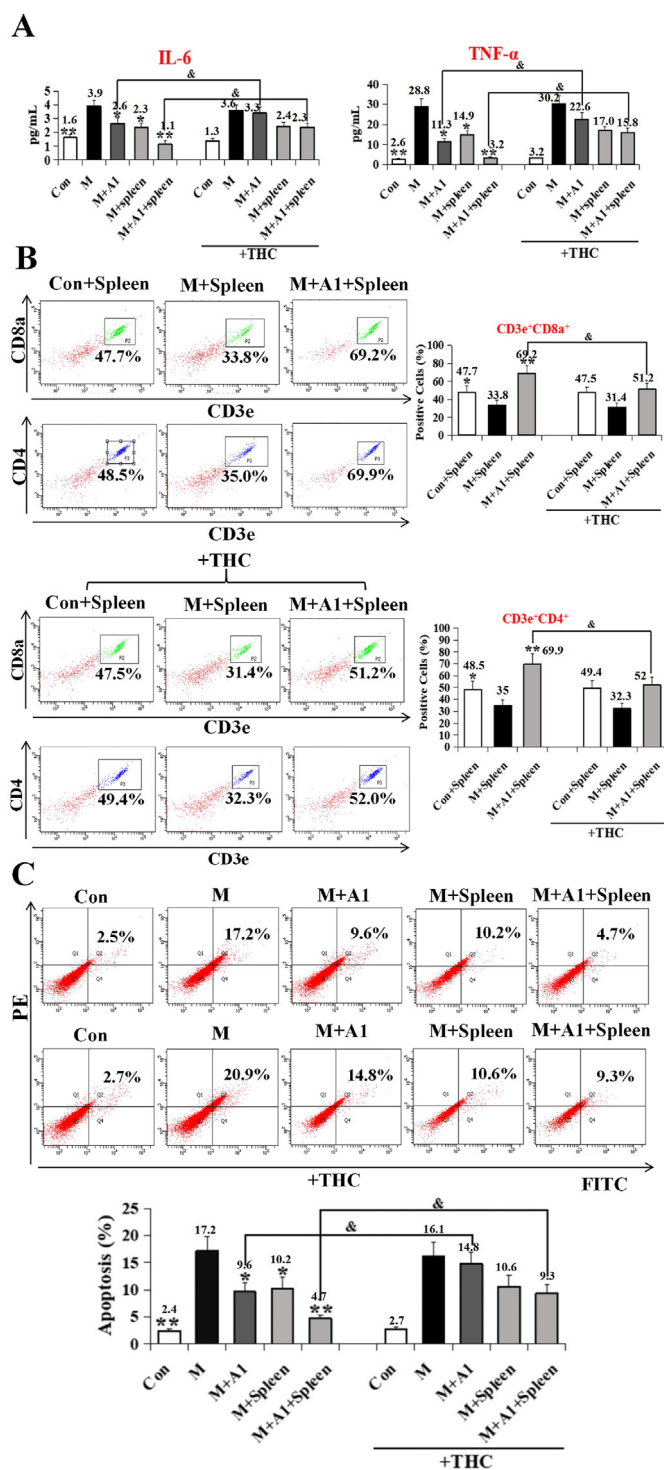


**Figure 6.** A1 (Corchoionol C) reprograms the microenvironment through ER $\beta$  in co-culture system. After treatment with A1 (20  $\mu$ M)/THC (1  $\mu$ M) for 24 h, supernatant, splenic lymphocytes and BEAS-2B cells were segregated. A: Levels of IL-6 and TNF- $\alpha$ . B: The percentage of Th and Tc cells. C: The percentage of apoptosis of BEAS-2B cells. Representative results of three independent experiments were shown, data are presented as mean  $\pm$  SD; \* $p$  < 0.05, \*\* $p$  < 0.01 vs. model or model + spleen group.

activity of natural products to treat ALI [28]. Natural products can inhibit inflammation, improve barrier function, and reduce oxidative stress by regulating important signaling pathways (e.g., NF- $\kappa$ B, MAPK, TLRs, PPAR- $\gamma$ , and adenosine A2A receptors), indicating that natural products have broad application prospects [29, 30].

In our study, a sesquiterpenoid (A1) was isolated from the stems and leaves of *Dioscorea opposita* Thunb. and was found to have a positive therapeutic effect on ALI. We hoped to identify compounds with potent anti-ALI efficacy from the stems and leaves of *Dioscorea opposita* Thunb., similar to the discovery of artemisinin from the traditional anti-malarial Chinese medicinal herb, Herba Artemisiae Annuae. Vitamin E, as an antioxidant that protects cell membranes, has been reported to have a positive effect on LPS-induced ALI; accordingly, vitamin E was used as a positive control drug in the present study. Our results demonstrate that A1 treatment improved PAAT and PET (animal ultrasound); ameliorated endotheliocyte edema, the decreased number of mitochondria, basal membrane thickening, and broken elastic lamina (electron microscopy); and reduced apoptosis in lung tissue (immunofluorescence), indicating that A1 significantly reduced LPS-induced lung injury in mice.

Lipopolysaccharide (LPS) is the main component of the outer membrane of Gram-negative bacteria, and its use for the induction of ALI in animal models has been widely reported. During ALI, the secretion of proinflammatory factors such as TNF- $\alpha$  and IL-6 increases sharply, promoting inflammation and leading to lung damage [31, 32]. Among these, TNF- $\alpha$  is the earliest proinflammatory factor involved in ALI, which mediates the recruitment of neutrophils and stimulates the release of more inflammatory factors from neighboring cells [33, 34]. In addition, TNF- $\alpha$  can also increase vascular permeability and facilitate the formation of pulmonary edema, thereby aggravating lung injury [35, 36]. The release of IL-6 triggers a systemic inflammatory response and can therefore be used as an important indicator of the severity of ALI [37]. Moreover, the 2-DG optical probe can be taken up by inflammatory tissues and quantitated using a near-infrared fluorescence imaging system [21]. Our results demonstrate that A1 treatment significantly decreased the fluorescence intensity of the 2-DG optical probe and the levels of proinflammatory factors such as TNF- $\alpha$ , IL-6, IFN- $\gamma$ , and IL-17 (ELISA), indicating that A1 reduced the levels of inflammation in LPS-induced mice. Further, LPS-induced inflammation is regulated by a variety of immune cells. Our results show that A1 significantly increased the percentage of Th cells, Tc cells, DCs, and NK cells in a dose-dependent manner, and decreased the percentage of MDSCs and Tregs in both the mouse spleen and blood as compared with the model group (flow cytometry), suggesting that A1 has excellent immunoregulatory efficacy.

In recent years, phytoestrogens with few side effects have emerged as a research hotspot due to their similar function to endogenous estrogen. Phytoestrogens can directly or indirectly act at estrogen receptors, activate estrogen signaling pathways, initiate transcription of downstream target genes, and exert biological effects [38]. Studies have shown that estrogen receptors are widely present in immune cells and directly or indirectly affect specific immune responses through changes in estrogen synthase, which mainly include enhancement of cellular and humoral immune responses and release of proinflammatory factors (e.g., IL-1 $\beta$ , IL-6, TNF- $\alpha$ ) [39, 40]. The results of immunofluorescence and western blotting show that A1 increased the expression level of ER $\beta$  and decreased that of IL-1 $\beta$  in lung tissue in a dose-dependent manner. Molecular docking indicates that A1 can bind to ER $\beta$ , suggesting that it is a potential ER $\beta$  agonist. Moreover, A1 significantly reduced angiogenesis in LPS-induced lung injury.

To determine the role of ER $\beta$  in the effect of A1 on lung injury, we blocked ER $\beta$  in the co-culture system using THC (a specific ER $\beta$  antagonist). The results show that blockade of ER $\beta$  diminished the ability of A1 to lower the levels of IL-6 and TNF- $\alpha$  (ELISA) and attenuated the A1-induced increase in the percentage of Th and Tc cells and decreased the percentage of apoptosis of BEAS-2B cells (flow cytometry). These data indicate that blockade of ER $\beta$  diminishes the effects of A1 on the injured lung microenvironment, suggesting that A1 may exert its anti-ALI effects through the ER $\beta$  pathway.

In summary, we isolated a sesquiterpene (A1) from the stems and leaves of *Dioscorea opposita* Thunb., a pure sesquiterpene (A1) was able to improve lung function and reduce lung damage in LPS-induced mice. Mechanistic data show that A1 regulated the immune system and

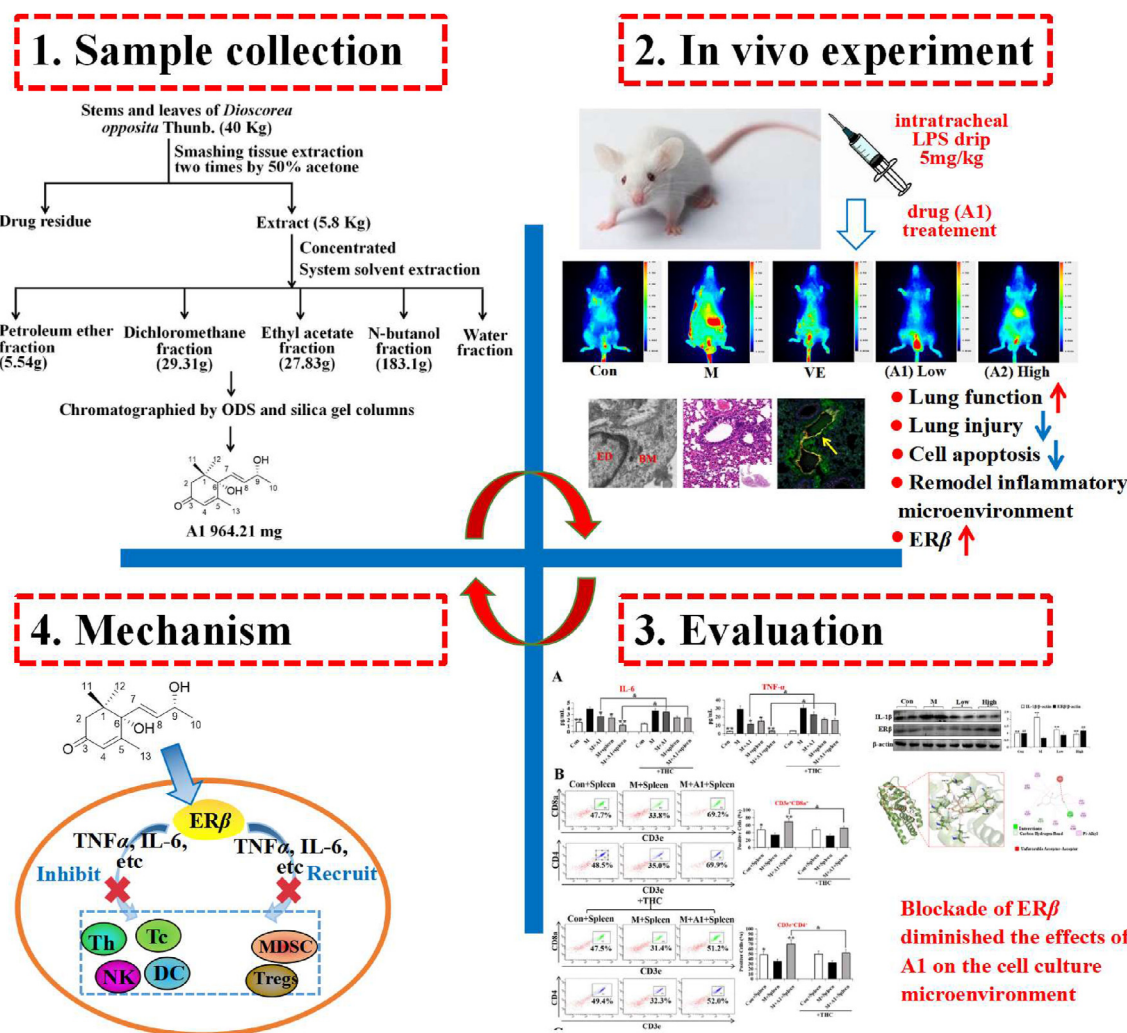


Figure 7. A schematic diagram showing the effects of A1 (Corchoionol C) in LPS-induced ALI.

decreased inflammation. Moreover, A1 increased the expression of ERβ in LPS-induced mice, and antagonism of ERβ decreased the protective effect of A1 in a co-culture system. Our results indicate that A1 had anti-ALI effects *in vivo*, which were partially mediated through ERβ signaling. We suggest that A1 has the potential to be developed as an alternative and/or complimentary agent for ALI management, which will simultaneously improve the comprehensive utilization rate of *Dioscorea opposita* Thunb.

**Declarations**

*Author contribution statement*

Mengnan Zeng: Conceived and designed the experiments; Analyzed and interpreted the data; Wrote the paper.

Beibei Zhang, Yingjie Ren: Performed the experiments; Analyzed and interpreted the data.

Shengchao Wang, Pengli Guo, Meng Liu, Qinqin Zhang, Jufang Jia, Jinyue Li: Performed the experiments.

Xiaoke Zheng, Weisheng Feng: Conceived and designed the experiments; Contributed reagents, materials, analysis tools or data.

*Funding statement*

This work was supported by the National Key Research and Development Project (2019YFC1708802, 2017YFC1702800), the Special

Project of Scientific Research on Traditional Chinese Medicine in Henan (20-21ZY2152), and the Doctoral Fund of Henan University of Chinese Medicine (RSBSJJ2019-10).

*Data availability statement*

Data will be made available on request.

*Declaration of interests statement*

The authors declare no competing interests.

*Additional information*

Supplementary content related to this article has been published online at <https://doi.org/10.1016/j.heliyon.2022.e10500>.

**References**

- [1] L. Hu, B. Wang, Y. Jiang, et al., Risk factors for transfusion-related acute lung injury, *Resp care* 66 (2021) 1029–1038.
- [2] M. Zhu, L. Wang, L. Yang, et al., Erythropoietin ameliorates lung injury by accelerating pulmonary endothelium cell proliferation via Janus Kinase-Signal transducer and activator of transcription 3 pathway after kidney ischemia and reperfusion injury, *Transplant. Proc.* 51 (2021) 972–978.
- [3] C. Huidobro, V.P. Martín, M.C. López, et al., Cellular and molecular features of senescence in acute lung injury, *Mech. Ageing Dev.* 193 (2021).

- [4] J.Y. Mao, D.K. Li, H.M. Zhang, et al., Plasma mitochondrial DNA levels are associated with acute lung injury and mortality in septic patients, *BMC Pulm. Med.* 21 (2021) 66.
- [5] B. Bayat, K.R. Nielsen, G. Bein, et al., Transfusion of target antigens to pre-immunized recipients: a new mechanism in transfusion-related acute lung injury, *Blood adv* 43 (2021).
- [6] D. Song, H. Chen, Trying to explain the theoretical basis of traditional Chinese medicine "Huashi Baidu Fang" in the treatment of coronavirus disease 2019 with western medical theory: a review, *Adv. Biosci. Biotechnol.* 11 (2020) 421–441.
- [7] G. Wu, W. Zhang, H. Li, Application of metabolomics for unveiling the therapeutic role of traditional Chinese medicine in metabolic diseases, *J. Ethnopharmacol.* 242 (2019), 112057.
- [8] K.C. Lan, S.C. Chao, H.Y. Wu, Salidroside ameliorates sepsis-induced acute lung injury and mortality via downregulating NF- $\kappa$ B and HMGB1 pathways through the upregulation of SIRT1, *Sci Rep-UK* 7 (2017), 12026.
- [9] X. Shi, G.N. Chen, J. Wei, UHPLC-Q-TOF MS based metabolic analysis for the therapeutic efficacy of "Xuebijing Injection" against sepsis-induced acute lung injury, *Evid-based Compl Alt.* 8 (2018), 8514619.
- [10] T. Nagai, N. Suzuki, N. Kai, et al., Functional properties of autolysate and enzymatic hydrolysates from yam tsukuneimo (*Dioscorea opposita* Thunb.) tuber mucilage tororo: antioxidant activity and antihypertensive activity, *J. Food Sci. Technol.* 51 (2014) 3838–3845.
- [11] S. Yu, B. Han, X. Bai, et al., The cold-soaking extract of Chinese yam (*Dioscorea opposita* Thunb.) protects against erectile dysfunction by ameliorating testicular function in hydrocortisone-induced KDS-Yang rats and in oxidatively damaged TM3 cells, *J. Ethnopharmacol.* 263 (2020).
- [12] R. Zhou, Y.H. Kang, Rheological properties and effects of in vitro gastrointestinal digestion on functional components and antioxidant activities of cooked yam flour, *Food Sci. Biotechnol.* 28 (2019) 991–1001.
- [13] X. Zhao, L. Yu, S.D. Zhang, Cryptochlorogenic acid attenuates LPS-induced inflammatory response and oxidative stress via upregulation of the Nrf2/HO-1 signaling pathway in RAW 264.7 macrophages, *Int. J. Immunopharm.* 83 (2020), 106436.
- [14] C.Y. Kwan, C.X. Chen, T. Deyama, et al., Endothelium-dependent vasorelaxant effects of the aqueous extracts of the *Eucommia ulmoides* Oliv. leaf and bark: implications on their antihypertensive action, *Vasc. Pharmacol.* 40 (2003) 229–235.
- [15] Y. Ren, M. Zeng, Y. Cao, A new diphenylethane and a new dibenz[b,f]oxepin with estrogenic activity from the stems and leaves of *Dioscorea oppositifolia* L., *Phytochem Lett* 33 (2019) 26–30.
- [16] Y. Ren, Y. Cao, M. Zeng, Two new norsesquiterpenoids with estrogenic activity from the stems and leaves of *Dioscorea oppositifolia* L., *Nat. Prod. Res.* 173 (2019) 1–8.
- [17] M. Zeng, L. Zhang, B. Zhang, et al., Chinese yam extract and adenosine attenuated LPS-induced cardiac dysfunction by inhibiting RAS and apoptosis via the ER-mediated activation of SHC/Ras/Raf1 pathway, *Phytomedicine* 61 (2019).
- [18] W. Xia, H. Zhang, Q. Zhou, et al., Inhibition of ER $\alpha$  aggravates sepsis-induced acute lung injury in rats via provoking inflammation and oxidative stress, *Oxid. Med. Cell. Longev.* 48 (2020).
- [19] X.J. Wu, Q. Kong, L.Y. Zhan, TIPE2 ameliorates lipopolysaccharide-induced apoptosis and inflammation in acute lung injury, *Inflamm. Res.* 68 (2020) 981–992.
- [20] H. Taizou, H. Toshiaki, T. Naoki, et al., OX40 ligand newly expressed on bronchiolar progenitors mediates influenza infection and further exacerbates pneumonia, *EMBO Mol. Med.* 8 (2016) 422–436.
- [21] M. Zeng, Y. Cao, R. Xu, et al., Oleanolic acid derivative isolated from *Gardenia jasminoides* var. *radicans* alleviates LPS-induced acute kidney injury in mice by reducing oxidative stress and inflammatory responses via the TLR4/NF- $\kappa$ B/NLRP3 signaling pathway, *New J. Chem.* 44 (2020) 2091.
- [22] Y.X. Liu, J.X. Bai, T. Li, et al., A TCM formula comprising *Sophorae Flos* and *Lonicerae Japonicae Flos* alters compositions of immune cells and molecules of the STAT3 pathway in melanoma microenvironment, *Pharmacol. Res.* 142 (2019) 115–126.
- [23] J. Beck, H. Engler, H. Brunner, et al., Interferon production in cocultures between mouse spleen cells and tumor cells, *J. Immunol. Methods* 38 (1980) 63–73.
- [24] Z. Liu, P. Wang, S. Lu, et al., Liquiritin, a novel inhibitor of TRPV1 and TRPA1, protects against LPS-induced acute lung injury, *Cell Calcium* 88 (2020), 102198.
- [27] F. Abedi, A.W. Hayes, R. Reiter, et al., Acute lung injury: the therapeutic role of Rho kinase inhibitors, *Pharmacol. Res.* 155 (2020), 104736.
- [28] Z. Ding, R. Zhong, T. Xia, et al., Advances in research into the mechanisms of Chinese Materia Medica against acute lung injury, *Biomed. Pharmacother.* 122 (2020), 109706.
- [29] Y.Q. He, C.C. Zhou, L.Y. Yu, et al., Natural product derived phytochemicals in managing acute lung injury by multiple mechanisms, *Pharmacol. Res.* 52 (2020).
- [30] M.G. Soliman, H.A. Mansour, W.A. Hassan, et al., Mesenchymal stem cells therapeutic potential alleviate lipopolysaccharide-induced acute lung injury in rat model, *J. Biochem. Mol. Toxicol.* 32 (2017), 22217.
- [31] A. Nadeem, S.F. Ahmad, N.O. Al-Harbi, et al., Inhibition of spleen tyrosine kinase signaling protects against acute lung injury through blockade of NADPH oxidase and IL-17A in neutrophils and  $\gamma\delta$  T cells respectively in mice, *Int. Immunopharm.* 68 (2019) 39–47.
- [32] A. Nadeem, N.O. Al-Harbi, S.F. Ahmad, et al., Blockade of interleukin-2-inducible T-cell kinase signaling attenuates acute lung injury in mice through adjustment of pulmonary Th17/Treg immune responses and reduction of oxidative stress, *Int. Immunopharm.* 83 (2020), 106369.
- [33] I.G. Ko, J.J. Hwang, B.S. Chang, et al., Polydeoxyribonucleotide ameliorates lipopolysaccharide-induced acute lung injury via modulation of the MAPK/NF- $\kappa$ B signaling pathway in rats, *Int. Immunopharm.* 83 (2020), 106444.
- [34] A. Nadeem, N. Siddiqui, N.O. Al-Harbi, et al., Acute lung injury leads to depression-like symptoms through upregulation of neutrophilic and neuronal NADPH oxidase signaling in a murine model, *Int. Immunopharm.* 47 (2017) 218–226.
- [35] A. Nadeem, N.O. Al-Harbi, S.F. Ahmad, et al., Glucose-6-phosphate dehydrogenase inhibition attenuates acute lung injury through reduction in NADPH oxidase derived reactive oxygen species, *Clin. Exp. Immunol.* 191 (2018) 279–287.
- [36] N.O. Al-Harbi, F. Imam, M.M. Al-Harbi, et al., Dexamethasone attenuates LPS-induced acute lung injury through inhibition of NF- $\kappa$ B, COX-2, and pro-inflammatory mediators, *Immunol. Invest.* 45 (2016) 349–369.
- [37] N.O. Al-Harbi, A. Nadeem, S.F. Ahmad, et al., Sulforaphane treatment reverses corticosteroid resistance in a mixed granulocytic mouse model of asthma by upregulation of antioxidants and attenuation of Th17 immune responses in the airways, *Eur. J. Pharmacol.* 15 (2019) 276–284.
- [38] D.L. Inés, Y.A. Maria, S.H. Albert, et al., Effects of dietary phytoestrogens on hormones throughout a human lifespan: a review, *Nutrients* 12 (2020).
- [39] Z. Fan, H. Che, S. Yang, et al., Estrogen and estrogen receptor signaling promotes allergic immune responses: effects on immune cells, cytokines, and inflammatory factors involved in allergy, *Allergol. Immunopathol.* 47 (2019) 506–512.
- [40] K. Sapania, K. Susan, Sex hormones regulate innate immune cells and promote sex differences in respiratory virus infection, *Front. Immunol.* 9 (2018) 1653.